

# Observing Solid Concentrations in a Vertical Hydraulic Transport System

Literature Survey

J. van Stappen

Literature Survey



# **Observing Solid Concentrations in a Vertical Hydraulic Transport System**

## **Literature Survey**

LITERATURE SURVEY

J. van Stappen

March 14, 2018



---

# Abstract

An important demand for the operation of a currently developed Vertical Transport System designed for solid transport is that insight of the location of solid concentrations inside the riser is available, this information is required for different reasons: Monitoring the propagation of solid concentrations will enable anticipation of the coming flow at the vessel, it is required for controlling the pumps, it will indicate where plugs are likely to be formed and furthermore it will indicate if the aimed production is achieved. It was therefore proposed to measure the concentration at the booster stations and predict the propagation of the solids through the riser, using pressure difference measurements is selected for this purpose. For the research that will be performed a scaled test setup will be available.

This literature survey is made in order to collect important information regarding this topic, started is with analyzing the principles of vertical transport. It has been found that the velocity of vertical transport of solids depends on the particle diameter and that there is no method yet to measure this parameter online in a vertical flow, this parameter therefore is an unknown input of the system. Literature about the hydraulic gradient of mixtures was evaluated too since the pressure drop will be used to determine the volumetric concentration inside the riser. For the contribution of solids multiple theories were evaluated, but no model was found covering the whole range of solids that will be tested with the test setup, which is why multiple theories need to be evaluated in order to find the best match with the performed measurements. Literature was found about the efficiency decrease of centrifugal pumps, related to the particle diameter. This gives an option to determine the particle diameter: Using the test setup it can be investigated whether the particle diameter can be determined by measuring the efficiency decrease of the pump.

The Ensemble Kalman filter is found to be suitable for large-dimensional nonlinear problems, and is chosen to be used for an observer of the solids concentrations in the Vertical Transport System. The effects of inflation and localisation on the performance of the Enkf can be evaluated. If the particle diameter is observable from the output of the Enkf, then it is possible to use Sequential Input and State Estimation to estimate this parameter. A different method to estimate the particle diameter can be to construct a physical model where this parameter is observable.



---

# Table of Contents

<b>Abstract</b>	<b>i</b>
<b>1 Introduction</b>	<b>1</b>
1-1 Survey Objective and Outline . . . . .	3
1-1-1 Vertical Hydraulic Transport . . . . .	3
1-1-2 Observer Algorithms . . . . .	3
1-1-3 Conclusion . . . . .	3
<b>2 Vertical Hydraulic Transport</b>	<b>5</b>
2-1 Vertical Hydraulic Transport Principles . . . . .	5
2-1-1 1D Vertical Hydraulic Transport model . . . . .	6
2-1-2 b1DVHT model . . . . .	7
2-1-3 Discussion . . . . .	7
2-2 Settling velocity . . . . .	7
2-2-1 Ruby & Zanke . . . . .	8
2-2-2 Ferguson and Church . . . . .	8
2-2-3 Hindered Settling . . . . .	8
2-2-4 Velocity gradient . . . . .	9
2-2-5 Discussion . . . . .	9
2-3 Nodule characteristics . . . . .	10
2-4 Hydraulic gradient . . . . .	11
2-4-1 Fluid wall shear stress . . . . .	12

2-4-2	Solid wall shear stress . . . . .	13
2-4-3	Discussion . . . . .	17
2-5	Riser Swaying . . . . .	17
2-6	On-line density Measurements . . . . .	18
2-7	Solids effect on Centrifugal Pumps . . . . .	20
2-7-1	Discussion . . . . .	21
2-8	Nodule degradation . . . . .	21
<b>3</b>	<b>Observer Algorithms</b>	<b>23</b>
3-1	The filtering problem . . . . .	23
3-2	Kalman Filter . . . . .	24
3-3	Extended Kalman Filter (EKF) . . . . .	25
3-4	Particle filter . . . . .	26
3-5	Unscented Kalman Filter (UKF) . . . . .	27
3-6	Ensemble Kalman Filter (EnKF) . . . . .	28
3-6-1	Undersampling . . . . .	30
3-6-2	Inbreeding . . . . .	31
3-6-3	Spurious Correlations . . . . .	31
3-6-4	Filter divergence . . . . .	31
3-7	Unknown Input Observer . . . . .	32
3-8	Simultaneous Input and State Filtering (SISF) . . . . .	33
3-9	Observers in Slurry Transport . . . . .	34
3-10	Cascade observers . . . . .	35
<b>4</b>	<b>Conclusion</b>	<b>37</b>
4-1	Vertical Hydraulic Transport . . . . .	37
4-2	Observer Algorithms . . . . .	38
	<b>Bibliography</b>	<b>39</b>
	<b>Glossary</b>	<b>43</b>

---

# Chapter 1

---

## Introduction

As the world's population rises and the application of electronics increases, the demand for rare earth metals such as Cobalt and Nickel grows. Deposits of these metals can be found on land but with the increasing demand there is a great probability that this will not be enough in the future. It therefore becomes interesting to investigate the possibility of mining these metals out of the sea.

In the 19th century it was found that in large areas in earth's oceans so called *polymetallic nodules* are present, these rock like objects are also called *manganese nodules* and contain concentrations of various rare earth metals. Manganese is the main component of the nodules, besides this they also contain various other metals of which nickel, copper, and cobalt are the most valuable [1]. Polymetallic nodules are formed by bacteria and consists of iron and manganese hydroxides, they are slowly formed, it is estimated that the diameter of a nodule increases with a rate of  $0.1\text{mm}$  per  $1000\text{years}$ , the nodules diameter of the nodules can be up to  $10\text{cm}$ .



**Figure 1-1:** Poly-metallic nodules laying on the see floor, source: IHC

Polymetallic nodules are formed in deep sea, large concentrations can be found at depths ranging from  $4000\text{-}6000\text{m}$ , the concentration of a field can be up to  $15\text{kg}/\text{m}^2$ . Figure 2-3 shows a field of nodules on the sea floor.

Currently a way to retrieve these nodules from the sea floor is being investigated by IHC. Besides developing a collector that harvests the nodules, a vertical transport system (VTS) is designed to bring the nodules to the sea level. The method of hydraulic transport is favoured by IHC for this purpose: Water is pumped upward in a riser using centrifugal pumps, at the bottom of the riser the solids are added and due to drag forces nodules are transported to the surface along with the carrying fluid. In Figure 1-2 a schematic representation of the riser is presented.

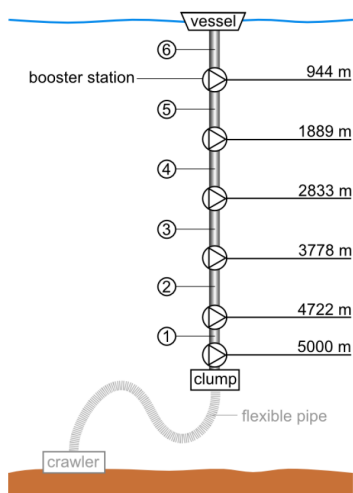


**Figure 1-2:** VTS schematization

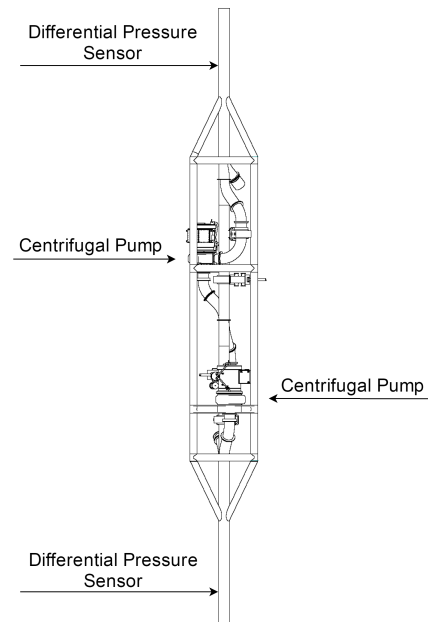


**Figure 1-3:** Booster station

As is seen in the figure the riser is divided into different riser sections, the sections have a length of 1000m. Between every riser section a booster station is present, which is shown in Figure 1-3. Every booster station contains two centrifugal pumps, these pumps are the driving force of the the vertical transport system.

An important demand for the operation of the VTS is that insight of the location of solid concentrations inside the riser is available, this information is required for different reasons: Monitoring the propagation of solid concentrations will enable anticipation of the coming flow at the vessel, it is required for controlling the pumps, it will indicate where plugs are likely to be formed and furthermore it will indicate if the aimed production is achieved. It is therefore proposed to measure the concentration at the booster stations and predict the propagation of the solids through the riser, using pressure difference measurements is selected for this purpose [2].

IHC has designed and built a test setup to investigate phenomena related to Vertical Hydraulic Transport of solids, experiments are conducted in a circuit that features a riser section of approximately 140m. In the circuit pressure difference sensors will be installed which make this an excellent set-up for investigating the observation of solid concentrations in a riser, the measurement data of this test program is used for this research.

## **1-1 Survey Objective and Outline**

The research goal is to accurately measure solid concentrations in a vertical hydraulic transport system. It has been determined that pressure difference measurements will be used to determine the concentration in the vertical transport system, this research will contain a measurement program with a scaled version of the vertical transport system where this principle will be tested. The goal of this literature survey is to address the properties of vertical transport, which are important to take into account for the observation system, and which can be investigated in the research. The literature survey is divided into three chapters of which the content is shown below:

### **1-1-1 Vertical Hydraulic Transport**

This chapter addresses the properties of Vertical Hydraulic Transport, the chapter starts with an elaboration of the basic principles hydraulic transport is based on. This is followed by models that are described in literature which can be used to simulate vertical transport. A section is dedicated to the characteristics of nodules, in order to understand the dimensions of the material that is transported. The transport velocity of the solids is affected by the size of the solids which is why the settling velocity of solids is investigated.

Since the concentration will be measured by means of pressure drop in the VTS, literature will be evaluated describing the effect of slurries on the hydraulic gradient which is a measure for the pressure drop. Furthermore the effect of movement of the riser on the pressure drop is investigated. Centrifugal pumps are an important aspect of the vertical transport system which is why the effect of solids on the pump performance is investigated as well.

### **1-1-2 Observer Algorithms**

The second chapter of this survey addresses observer algorithms that are suitable for slurry transport. Since models describing Vertical Hydraulic Transport contain non-linear relations, non-linear observers are elaborated, and since the VTS is discretised in many states an observer suitable for large dimensional systems is investigated. It will be furthermore investigated how unknown inputs can be observed, literature where this has been done applied to the transport of slurries is elaborated as well.

### **1-1-3 Conclusion**

This chapter will provide a summary of what is found in literature, concluding with recommendations for the research.



# Vertical Hydraulic Transport

An introduction to hydraulic transport is provided in this chapter, followed by two models that can be used to simulate vertical transport. An elaboration follows about the material transported (manganese nodules), and the settling velocity which is a result of the characteristics of the solids. Slurry will have an effect on the pressure difference measurements, which is elaborated in the sections following up. This chapter ends with an chapter about the effect of slurry on centrifugal pumps which can also be used to measure slurry aspects.

## 2-1 Vertical Hydraulic Transport Principles

The principles of hydraulic transport are elaborated in this section. The aim of the research is to gain knowledge about the occupation of solids inside the riser, this parameter is expressed as the volumetric concentration. The volumetric concentration represents the volume in a section of the riser that is occupied with solids, as a fraction of the total volume of that section. In equation 2-1 the volumetric concentration is expressed using the solid density  $\rho_s[\frac{kg}{m^3}]$ , the fluid density  $\rho_f[\frac{kg}{m^3}]$  and the mixture density  $\rho_m[\frac{kg}{m^3}]$ .

$$c_v = \frac{\rho_m - \rho_f}{\rho_s - \rho_f} \quad (2-1)$$

The volumetric concentration is a measure used for quantifying solid concentrations in the VTS riser. Propagation of this concentration needs to be monitored and therefore the different velocities that are related are important. Considering a section of the riser one can distinguish the velocity of the carrying fluid (the fluid velocity ( $v_f[\frac{m}{s}]$ )) and the velocity of the solids propagating (solid velocity ( $v_s[\frac{m}{s}]$ )). Between these two parameters there is a hindered settling velocity ( $w_h[\frac{m}{s}]$ ). Figure 2-1 represents the different velocities in the mixture. 2-1.

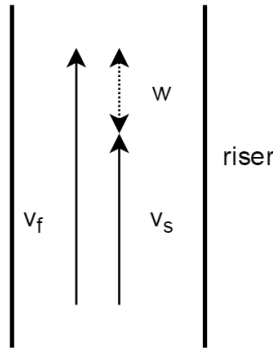


**Figure 2-1:** Different velocities in a riser

The settling velocity  $w_h$  depends on the particle diameter and the local volumetric concentration. Fractions of different particles will have different settling velocities and will therefore travel with a different solid velocity than fractions of other sizes. The bulk mixture velocity is constant throughout the whole riser, and is defined as the cross sectional average velocity of the volume flow:

$$\bar{v}_m = c_v \cdot v_s + (1 - c_v) \cdot v_f \quad (2-2)$$

The solid velocity  $v_s$  and fluid velocity  $v_f$  can then be written as a combination of the mixture velocity and the the settling velocity:

$$v_s = \bar{v}_m + c_v \cdot w_h - w_h \quad (2-3)$$

$$v_f = \bar{v}_m + c_v \cdot w_h \quad (2-4)$$

A very important property for the propagation of solids is the hindered settling velocity which depends on the solid characteristics and the volumetric concentration.

### 2-1-1 1D Vertical Hydraulic Transport model

A thesis has been dedicated investigating the vertical transport of manganese nodules [3]. In this thesis it has been proven that it is possible that plug formation can occur in a riser where multiple solids fractions are present.

Part of the work done for this thesis is the creation of the 1DVHT model *1D vertical hydraulic transport model*. The model simulates propagations of solids concentrations in one dimension driven by a vertical flow of water. It takes into account the effect of multiple fractions of particle diameters present in the flow. The advection-diffusion equation is solved:

$$\frac{\partial c_v}{\partial t} + \frac{\partial c_v v_s}{\partial z} = \frac{\partial}{\partial z} \left( \epsilon_z \frac{\partial c_v}{\partial z} \right) \quad (2-5)$$

In this equation  $z$  is pointed upward, states are discretised over the length of the riser. The output of the model is the mixture bulk velocity, the pressure distribution, and the concentration at the discretised riser segments.

The momentum equation is solved using the implicit Adam-Bashfort 2-time integration scheme, the pressure distribution is then solved using a succesove overrelaxation method. The result is a nonlinear model with states representing the volumetric concentration spatially discretised. Outcome of the model has been verified by making use of a sedimentation test, the results have shown good agreement between the model and the experiments.

### 2-1-2 b1DVHT model

Incorporating the full IDVHT model into an observation algorithm results in a set of calculations that require too much computational power to run real-time. It has been investigated how the complexity of the model can be decreased. Simplifications of the model have been investigated [2], The simplifiactions aim on reducing the computational power needed while maintaining a model that approaches the output of the 1DVHT model. The simplified model is called the b1DVHT model (basic 1D Vertical Hydraulic Transport) and it uses the same equations to solve the advection-diffusion equation.

In the basic model the PSD of the particles is represented as a reduced PSD of around 2 representative solid fractions. Mixture friction factors are assumed constant, and furthermore the mixture velocity update is changed from an implicit to an explicit scheme.

### 2-1-3 Discussion

It has been shown that the b1DVHT model resembles the 1DVHT model very well if the right particle diameter fractions are considered. However for these experiments the 1DVHT model was simulated at a PSD that equals the PSD of the manganese nodule field, during the collecting of nodules the size of the particles entering the VTS will not be according to this PSD at all times. It is therefore an important addition to the observer to estimate the particle diameter as well, since this parameter is varying and depending on what is collected at the sea bed this parameter is considered to be an unknown input of the system.

An important effect of different particle diameters is the settling velocity which determines the velocity of the solids through the riser, this parameter will be investigated in the next sections.

## 2-2 Settling velocity

Particles will not move in the same velocity as the fluid. The difference in velocity between these two parameters is called *slip*. The slip velocity is calculated as follows:

$$w_h = v_f - v_s \quad (2-6)$$

This phenomenon is created by the particle's tendency to settle which is related to the maximum velocity a particle will fall in still water, the terminal settling velocity  $w_t$ . The particle Reynolds number determines whether this process is turbulent or laminar:

$$Re_p = \frac{w_t \cdot d}{\nu_f} \quad (2-7)$$

In which  $d[m]$  is the particle diameter and  $\nu_f$  is the kinematic viscosity  $\nu_f[m^2/s]$ .

### 2-2-1 Ruby & Zanke

An equation for the settling velocity in the transition regime between laminar and turbulent ( $1 < Re_p < 2000$ ), has been derived by Ruby & Zanke [4].

$$w_t = \frac{10 \cdot \nu_f}{d} \cdot \left( \sqrt{1 + \frac{\frac{\rho_s - \rho_f}{\rho_f} \cdot g \cdot d^3}{100 \cdot \nu_f^2}} - 1 \right) \quad (2-8)$$

### 2-2-2 Ferguson and Church

A different equation has been developed by Ferguson and Church in order to provide a continuous formula covering the different regimes [5], and thus particle sizes:

$$w_t = \frac{\rho_s - \rho_w}{\rho_w} g d^2 \left( C_1 \cdot \nu_f + [C_2 \cdot 0.75 \frac{\rho_s - \rho_w}{\rho_w} g d^3]^{0.5} \right)^{-1} \quad (2-9)$$

The equation incorporates the Stokes law for small grains and a constant drag coefficient for large grains. Parameters  $C_1$  and  $C_2$  can be selected for different types of solids. A configuration of parameters as proposed in the original paper is shown in table 2-1:

**Table 2-1:** Grain shape parameters, source: [5]

Material	$C_1$	$C_2$
Smooth spheres	18	0.4
Natural sands	18-20	1-1.1
Very angular grains	24	1.2

### 2-2-3 Hindered Settling

If the concentration of solids in the mixture increases, the settling velocity will decrease. This effect is created by an increased liquid volume flow going up due to the settling volume of solids. The hindered settling velocity is defined as:

$$w_h = w_t \cdot (1 - c_v)^n \quad (2-10)$$

The exponent  $n_{rz}$  can be approximated with the following equation [6]:

$$n_{rz} = \frac{4.7 + 0.41Re_p^{0.75}}{1 + 0.175Re_p^{0.75}} \quad (2-11)$$

When the settling velocity is considered with respect to the fluid velocity instead of the mixture velocity the exponent  $n_{rz}$  needs to be replaced by  $n_{rz} - 1$  to correct for the frame of reference.

#### 2-2-4 Velocity gradient

For particle settling in vertical pipes the the ratio of the particle diameter compared to the pipe diameter needs to be taken into account. Fluidization experiments have shown that the settling velocity scales with  $10^{-\frac{d}{D}}$ , The equation then becomes [7]:

$$w_h = 10^{-\frac{d}{D}} w_t (1 - c_v)^n \quad (2-12)$$

#### 2-2-5 Discussion

In the test program of this research tests will be performed with solids that have diameters ranging from 0–10mm. If the Ruby and Zanke equation is considered for the settling velocity of the 10mm particles that would result in a particle Reynolds number of approximately 3000, that would be out of the transitional regime. This formula is therefore not suitable for the tests.

The Ferguson and Church equation was selected to be used for the 1DVHT model and will also be suitable for the experiments that will be conducted. Experiments performed in the original paper have shown agreement for solids of  $d = 0.068mm - 4.35mm$ . Solids used in the experiments of this research will consist of mixtures of sand and gravel, the solid type is therefore considered to be somewhere in between natural sand and very angular material. For the experiments  $C_1 = 22$  and  $C_2 = 1.1$  is selected.

The relation for the terminal settling velocity is an empirical relation. For solids of 4.36mm the standard deviation of the measurements is roughly 1%, however this value is determined in still water which is not the same as as in a turbulent flow. Furthermore the equation for the hindered settling velocity is an extension using findings of two other researches. Considering the fact that 10mm will also be an extrapolation of this equation it is clear that the witnessed hindered settling velocity in the experiments may deviate.

Fluidization experiments of [3] have been analysed [2] in order to find whether the theories for settling and hindered settling combined yield good results, for particle diameters of 10–35mm the results were matching well but resulted in an overestimation for large concentrations and an underestimation for low concentrations. Furthermore the spread found was relatively large. It is concluded that the settling velocity can be approximated but that it is not precisely known.

## 2-3 Nodule characteristics

Solids to be transported in the VTS are the poly-metallic nodules. Important parameters to be known for the settling velocity are the size, shape and density of the nodules, a research has been carried out investigating these properties of the manganese nodules [8]. For this research nodules have been used that are collected during cruises of the German research ship *Valdivia*. In Table 2-2 density of nodules are depicted measured from samples collected during cruises of this ship. The samples are taken from cruises in the western part of the manganese nodule belt (about 1000 sea mile south-east of Hawaii).

**Table 2-2:** Mean values of solid density, dry bulk density, wet bulk density and porosity of manganese nodules [8]

	Mean value	minimum	maximum	standard deviation
Solid density [ $g/cm^3$ ]	3.334	3.054	3.526	0.136 (4.1%)
Dry bulk density [ $g/cm^3$ ]	1.396	1.217	1.646	0.069 (4.9%)
Wet bulk density [ $g/cm^3$ ]	1.99	1.94	2.08	0.03 (1.5%)
Porosity [Vol -%]	58.31	55.20	62.64	1.93 (3.3%)

It can be seen that the nodules are very porous. During vertical transport the nodules will remain wet which is why only the solid density will be important for this research. The variation of density of the nodules depends on the composition of metals inside, The small standard deviation teaches that the difference between wet-densities through a field is little.

However, densities of nodules can be different at other locations. At the Clarion-Clipperton zone a mean wet nodule density of  $2,150 kg/m^3$  is found [9], this has been the reference for the Blue Mining program. At this location also a rough estimate of the Particle Size Distribution (PSD) is made, this distribution is shown in figure 2-2. The distribution is made using different sieve sizes.

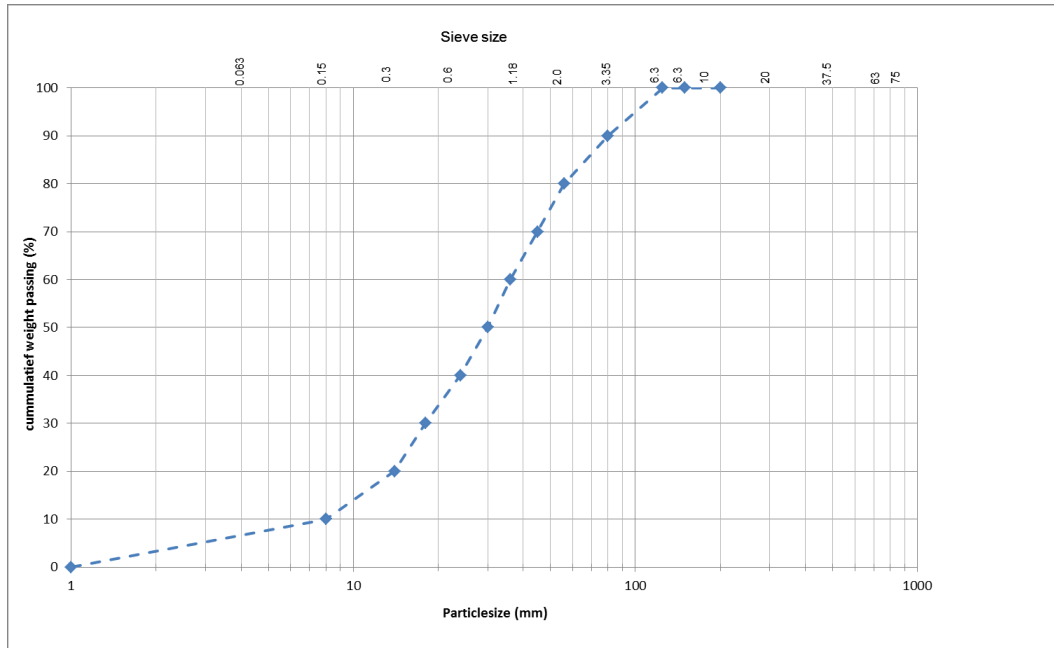


Figure 2-2: Nodule sizes in the Clarion-Clipperton zone

It can be seen that the nodule size ranges from 0-100mm and that the mass-median lies around a particle size of 30mm. This means that 50% of the mass of nodules in a field consists out of particles ranging from 0-30mm. In that region there is a large difference in settling velocity for the particle diameters which confirms that it is valuable information to know the particle diameter in the slurry flow.

## 2-4 Hydraulic gradient

As proposed the volumetric concentration of solids in the VTS will be determined using the pressure difference measurements [2]. The pressure drop over a vertical section of a riser is a summation of the static weight of the mixture and the pressure drop created by wall shear stress. A term used to quantify the pressure drop is the hydraulic gradient, the hydraulic gradient (dimensionless) relates the pressure drop of a mixture to the static weight of the carrying fluid. The total hydraulic gradients ( $i_t$ ) is related to the pressure in the following way:

$$i_t = \frac{\Delta p}{\Delta z} \frac{1}{\rho_f g} \quad (2-13)$$

The hydraulic gradient is a summation of gradient created by the potential energy  $i_p$ , the gradient induced by wall friction of the solids  $i_s$  and the gradient induced by wall friction of the carrying fluid  $i_f$ :

$$i_t = i_p + i_f + i_s \quad (2-14)$$

The gradient due to potential energy is defined as:

$$i_p = c_v \cdot \left( \frac{\rho_s}{\rho_f} - 1 \right) + 1 \quad (2-15)$$

The other terms  $i_f$  and  $i_s$  are a result of two wall shear stresses: the fluid wall shear stress  $\tau_f$  and the solid wall shear stress  $\tau_s$ , the summation of these terms yields the mixture shear stress:

$$\tau_m = \tau_f + \tau_s \quad (2-16)$$

This wall shear stress works parallel on the pipe wall, the pressure drop over a section is thus defined by the force created by the wall shear stress of the pipe wall divided by the cross section of the pipe:

$$\Delta p = \frac{F}{A_p} = \frac{\tau_m \cdot \pi \cdot D \cdot \Delta z}{\frac{\pi}{4} \cdot D^2} = 4 \cdot \tau_m \cdot \frac{\Delta z}{D} \quad (2-17)$$

### 2-4-1 Fluid wall shear stress

The wall shear stress for the fluid is expressed using the Darcy-Weisbach friction factor  $f_D$ :

$$\tau_f = \frac{1}{8} \cdot f_D \cdot \rho_f \cdot v_f^2 \quad (2-18)$$

So for fluids the pressure drop created by wall shear stress equals:

$$\Delta p = 4 \cdot \tau_f \cdot \frac{\Delta z}{D} = f_d \cdot \frac{1}{2} \cdot \frac{\Delta z}{D} \cdot \rho_f \cdot v_f^2 \quad (2-19)$$

The friction factor  $f_D$  for the turbulent regime can be approximated using the Swamee Jain equation [10]. The Wall friction depends on the pipe diameter ( $D$ ), the wall roughness ( $\epsilon$ ) and the Reynolds number ( $Re_f$ ):

$$f_D = \frac{1.325}{\left( \ln \left( \frac{\epsilon}{3.7 \cdot D} + \frac{5.75}{Re_f^{0.9}} \right) \right)^2} \quad (2-20)$$

Where the Reynolds number is defined as:

$$Re = \frac{v_f \cdot D}{\nu_f} \quad (2-21)$$

### 2-4-2 Solid wall shear stress

For mixtures the contribution of solids to the pressure drop is calculated as follows:

$$\Delta p = 4 \cdot \tau_s \cdot \frac{\Delta z}{D} \quad (2-22)$$

The solid wall shear stress has been widely investigated and found literature is elaborated in the next sections.

#### Equivalent Liquid Model

For a turbulent flow ( $Re > 2320$ ) vortices will exist close to the pipe wall, these are called the eddies. If the solids are very fine they can be considered to be part of the eddies, in that case the viscosity of the fluid is increased. In the Equivalent Liquid Model the wall shear stress is be considered to scale with the increase of density created by the solids:

$$\tau_m = \tau_f + \tau_s = \frac{\rho_m}{\rho_f} \cdot \tau_f \quad (2-23)$$

The limiting particle diameter for which the assumption can be made that the particles have an effect on the fluid viscosity can be approximated [11]:

$$d = \sqrt{\frac{Stk \cdot 9 \cdot \rho_l \cdot \nu_l \cdot D}{\rho_s \cdot v_f}} \approx \sqrt{\frac{Stk \cdot 9 \cdot \rho_l \cdot \nu_l \cdot D}{\rho_s \cdot 7.5 \cdot D^{0.4}}} \quad (2-24)$$

When larger particles are considered the Equivalent Liquid Model no longer holds.

#### Magnus effect

When the velocity gradient in a pipe is very steep and the particles are relatively large, particles will be pushed away from the pipe wall. Due to the steep velocity gradient the velocity will be lower at the side of the pipe, causing that at this side of the particle the pressure is larger which pushes the particle to the center. Furthermore the velocity gradient will cause the particle to spin which increases pressure difference due to the Magnus effect. The particle will tend to rotate and to move towards the axis of the pipe [11], and therefore the wall friction created by large solids may be less than the wall friction for smaller particles. The effect creates a lubrication of water in between the particle and the pipe wall.

#### Bagnold's number

A term used in some models for the hydraulic gradient is the Bagnold number (Ba). This number represents the ratio of grain collision stresses to viscous fluid stresses in a granular flow with interstitial Newtonian fluid [11]. The Bagnold number is defined as:

$$Ba = \frac{\rho_s \cdot d^2 \cdot \lambda^{1/2} \cdot u_*^2}{\rho_f \cdot v_f^2} \quad (2-25)$$

In this equation  $u_*$  is the shear velocity defined as:

$$u_* = \sqrt{\frac{f_D}{8}} \cdot v_f \quad (2-26)$$

In equation 2-25,  $\lambda$  is the linear concentration, this value is a measure of the particle diameter related to the distance to neighbouring particles [11]:

$$\lambda = \frac{1}{\left(\frac{c_{vmax}}{c_v}\right)^{1/3} - 1} \quad (2-27)$$

When the Bagnolds number is low ( $Ba < 40$ ), viscous fluid stresses dominate grain collision stresses, and the flow is said to be in the macro-viscous regime. The grain-inertia regime is found at a large Bagnold number ( $Ba > 450$ ). In this regime grain collision stresses dominate the wall friction.

### Shook & Bartosik

In 1994 a formula for the wall shear stress influenced by particles is presented by Shook and Bartosik [12]. Experiments have been conducted using solids with particle diameters between 1.37 and 3.4mm, in pipes with a diameter of 26 and 40mm. The experiments were conducted under conditions where slip between the particles and the fluid was very small, compared to the mean velocity. Using the experimental data, the following formula is proposed for the solid shear stress:

$$\tau_s = 102 \cdot Re_f^{-1.8} \rho_s d^2 \lambda_b^2 \gamma_f^2 \quad (2-28)$$

It was concluded that the wall friction in turbulent vertical flow is significantly influenced by the particles if the particles are larger than 1.5mm. Furthermore The wall stresses due to particles appear to be related to those discovered by Bagnold for Couette shear flow. It is also found that at high velocities the lubrication force between the wall and the particles becomes noticeable, resulting in a decrease of the solid wall shear stress  $\tau_s$ .

### Ferre & Shook

In 1998 experiments have been performed using spherical glass particles transported in a vertical flow loop with an internal pipe diameter of 40.9 mm. Particle diameters of 1.8 and 4.6mm have been investigated in concentrations ranging from 9% to 38%. The carrying fluids tested were water and ethylene glycol solutions, the contribution of the wall friction was found to be:

$$\tau_s = 0.0214 \left( \frac{\rho_s \bar{v}_m d}{\mu_f} \right)^{-0.36} \left( \frac{d}{D} \right)^{-0.99} \lambda^{1.31} \rho_s \bar{v}_m^2 \quad (2-29)$$

It has been concluded that wall shear stresses created by particles in vertical slurry flows is related to the formula found by Bagnold. It was also concluded that conditions under higher fluid viscosities would be useful, however this is of not interest for the that is considered VTS.

### Matousek

In 2009 tests have been carried out by Matousek [13]. Sand fractions with diameters of 0.12, 0.37 and 1.84 were analysed in a vertical pipe with a diameter of 150mm. In the tests it was found that the contribution of the solids to the wall stress is only negligible if the concentration is very low. It was found that the solids effect ( $i_s$ ) was larger for the small particle fraction than for the medium fraction. But it was also found that this effect in the largest fraction was smaller than in the smallest fraction. It was suggested that this result is due to the Magnus effect that has a larger influence on the medium solids fraction that were tested. Three correlations for the hydraulic gradient are found, for the different types of solids, for fine sand (0.12mm) the following relation is found:

$$\tau_s = \frac{5.47 c_{vd}^{1.14}}{v_m} \cdot \rho_f \cdot u_*^2 \quad (2-30)$$

And for medium sand (0.37mm):

$$\tau_s = \frac{31.8 c_{vd}^{2.45}}{v_m^{5.08} c_{vd}} \cdot \rho_f \cdot u_*^2 \quad (2-31)$$

And for coarse sand (1.84mm):

$$\tau_s = \frac{c_{vd}^{1.39}}{v_m^{-0.94} c_{vd}} \cdot \rho_f \cdot u_*^2 \quad (2-32)$$

In the research of Matousek it has been concluded that the solid contribution to the pipe wall shear stress can not be neglected when the volumetric concentration is above 10%. It is also concluded that the solids effect is strongly influenced by the off-wall lift force on the particles. This relation depends on the particle diameter with respect to the fluid velocity and pipe diameter. The fluid velocity has a larger effect on this than the particle diameter.

### Bartosik

Using a collection of data from previous researches a new formula for solid wall shear stress is presented in 2010 by Bartosik [14]. Data covers measurements of slurries containing particles ranging from 1-5mm, solid densities ranging from 1045 – 3000kg/m<sup>3</sup>, and volumetric concentrations ranging from 20-40%. This time the solid shear stress is expressed with respect to the fluid shear stress. A mathematical model was created using Bagnold's concept, the following relation was found:

$$\tau_s = \tau_f \cdot \left( (B_b D^2) \rho_p d^2 \lambda^{3/2} \frac{D}{4\mu_l^2} i_f \rho_f g \right) \quad (2-33)$$

In the tests it was found that the particle diameter  $d$  has a large effect on the particle wall stress. Also the solid concentration is important, but it was found that this starts to play a role when volumetric concentrations exceed 20%. The density of the solids was found to be of less influence.

Only small particles are tested which causes that for larger particles, where for example the slip velocity is more dominant the model might not predict the friction correctly. It is argued that the model is likely not suitable for coarse particles lower than 1.5 mm and higher than 5 mm.

## XIA

A relation for the hydraulic gradient of manganese nodules is presented by Xia [15], this collision model for the solids brings in some complicated formula. While it is likely that this contribution is rather small due to the Magnus effect, it has been recommended by Wang and Fei [16] to incorporate this effect when solid concentrations larger than 4% are present. The following formula for the hydraulic gradient created by solid collision is derived:

$$i_s = \frac{\gamma t_u}{\rho_m g L_u} \quad (2-34)$$

In this equation  $t_u$  is unit of time and  $L_u$  is unit of length.  $\gamma$  is the energy loss, and is calculated as the collision ( $N_c$ ) number times the amount of energy lost for each collision ( $\Delta E$ ). Expressed as follows:

$$N_c = \frac{1}{\sqrt{2}} \pi d_r^2 v_s \left( \frac{6c_v}{\pi d_r^3} \right)^2 \quad (2-35)$$

Where  $d_r$  is the representative diameter used for the solids. The second term evaluated is the energy loss for each collision:

$$\Delta E = \frac{1}{2} \frac{m_i m_j}{m_i + m_j} (e^2 - 1) u_{ij}^2 \quad (2-36)$$

In this equation  $m_i$  and  $m_j$  are the masses of two particles, with corresponding velocities  $u_i$  and  $u_j$  and particle sizes  $d_i$  and  $d_j$ .  $e$  is the restitution coefficient, the average velocity  $u_{ij}$  is determined according to the following formula:

$$u_{ij} = 0.2v_f + \frac{2}{3} \frac{d_i^2 - d_j^2}{D^2} v_{max} \quad (2-37)$$

$v_{max}$  is the flow velocity in the centerline of the pipe, Combined this yields for  $\gamma$ :

$$\gamma = \frac{\pi}{4\sqrt{2}} d_r^2 N^2 v_m (1 - e^2) \sum_{i,j=1}^n x_i \frac{m_i m_j}{m_i + m_j} u_{ij}^2 (i \neq j) \quad (2-38)$$

$x_i$  is the percentage weight corresponding to the particle size  $d_i$ . The calculation is done with several groups of nodules ( $n$ ) according to the nodule-size distribution, with corresponding mass and size. These equations form the hydraulic gradient due to particle collision. Test data was used covering concentrations ranging from 1.6%-15%, under mixture flow velocities of 1.5-4.1m/s. Model predictions were shown to agree with measured data.

### 2-4-3 Discussion

Different models were found in literature, an overview of the different regimes of the tests is provided in table 2-3.

**Table 2-3:** Used parameters in literature

Research	d [mm]	D [mm]	Max. $c_v$ [-]
Shook & Bartosik	1.37,1.5,3.4	26,40	45%
Ferre & Shook	1.8,4.6	40.9	38%
Matousek	0.12, 0.37,1.84	0.0008-0.012	43%
Bartosik	1-5	26	40%
Xia	15	100	15%

For the experiments that are performed for this research solids are used with a particle diameter ranging from  $1mm-10mm$ , the riser diameter is  $150mm$ . Except for the experiments of Matousek the particle diameter range in the planned setup is partly covered by the models elaborated in literature.

Most of the researches have been build on previous researches but the paper of Xia uses an model structure that is totally new. The fact that this model yields good results for the dataset he used is not considered to be a solid proof.

The models based on the linear concentration number might be suitable for the conditions of the test setup, but it can be argued that they are not applicable for large particle diameters. The linear concentration increases rapidly as the volumetric concentration approaches the maximum concentration because it represents the amount of particle interaction. However for very large particles a high volumetric concentration does not have to mean a large amount of particles. The models using this parameter might therefore not be suitable for slurry flows where the particle diameter is very large compared to the pipe diameter.

The models found in literature need to be compared in the research in order to select the one that best matches the measurements.

## 2-5 Riser Swaying

Theories for the hydraulic gradient of the flow have been elaborated in the last section. However these formulas are based on the assumption that the riser is completely vertical. At sea waves and currents interact with the ship and with the riser which result in oscillations of the system.

The effect of the swaying of the riser on the hydraulic gradient has been investigated [17]. Experiments have been conducted with a hydraulic lifting system with has a length of  $L = 10m$  and an internal diameter of  $50mm$ . A 4in. slurry pump was used with a controllable speed. The riser is hinged at the top, and swayed at the bottom. Nodules with a density of  $\rho_s = 2000kg/m^3$  and a mean diameter of  $10mm$  were used. Frequencies of 0.2, 0.4 and 0.6Hz were combined with amplitudes of 0.15, 0.25 and 0.4m, These conditions were tested with mixture flow velocities ranging from  $1.2 - 4.0m/s$ .

The effect of the swaying action of the pipe on the hydraulic gradient induced by the mixture is quantified through the following hydraulic gradient change parameter:

$$R_m = \frac{i_t}{i_{t0}} \quad (2-39)$$

In this formula  $i_t$  is the measured gradient during the swaying experiments and  $i_{t0}$  is the gradient measured when the riser is static. In the experiments it has been observed that the hydraulic gradient in a swaying pipe was larger than that of a static pipe. It has also been discovered that the hydraulic gradient is influenced by the mixture flow velocity, swaying amplitude, and swaying frequency. the main reason for the increment of the hydraulic gradient appears to be the enhancement of the particle-wall collisions by the swaying motion of the pipe. Values for  $R_m$  have been found in the range  $1 < R_m < 1.65$  which means the pipe swaying effect on the hydraulic resistance can be significant. A mathematical model was created that incorporates the pipe dynamics for the determination of the hydraulic gradient In [17].

In the planned test setup this effect cannot be investigated but it is interesting to see what will be the effect for the real VTS. Motions of the IHC designed VTS have been investigated [18], the frequencies and amplitudes are similar to the values investigated in the research. However the  $d/D$  ratio is significantly different, in the research values of  $10mm/50mm$  were investigated where in the design for the full scale VTS values of  $30mm/356mm$  are expected. The size of the nodules will be smaller compared to the pipe in the VTS of IHC, this means that the outcome of the research cannot be used directly, other than providing a recommendation to investigate this phenomena.

## 2-6 On-line density Measurements

A method for on-line measuring the slurry density in a vertical pipe section and avoiding the estimation of the wall shear stress is known [19]. This method requires that an up going and down going pipe section is present in the circuit as is shown in figure 2-3.

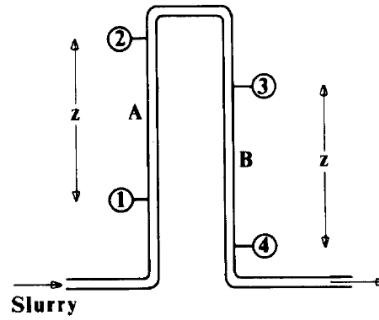


Figure 2-3: Measurement loop, source: [19]

Vertical pipe sections  $A$  and  $B$  are considered with corresponding wall shear stress  $\tau_{mA}, \tau_{mB}$  and corresponding mixture density  $\rho_{mA}, \rho_{mB}$ . Measuring the pressure at the four points indicated the following can be derived:

$$\begin{aligned} p_1 - p_2 &= zg\rho_{mA} + 4\tau_{mA}z/D \\ p_4 - p_3 &= zg\rho_{mB} - 4\tau_{mB}z/D \end{aligned} \quad (2-40)$$

If the assumption is made that  $\tau_{mA} = \tau_{mB}$ , which can be done since the bulk mixture velocity is equal in both parts, the wall shear stress is canceled out of the next equation:

$$\rho_{mA} + \rho_{mB} = [(p_1 - p_2) + (p_4 - p_3)]/zg \quad (2-41)$$

From the density the summation of concentrations can be expressed:

$$c_{vA} + c_{vB} = \left[ \frac{(p_1 - p_2) + (p_4 - p_3)}{zg} - 2\rho_f \right] (\rho_s - \rho_f) \quad (2-42)$$

The difference between  $c_{vA}$  and  $c_{vB}$  is created by the effect of the settling velocity. The equation can be solved to find the delivered volumetric concentration ( $c_{vd}$ ) through the two sections:

$$c_{vA} + c_{vB} = 2c_{vd} \left[ 1 + \frac{w_h^2}{v_m^2} \left( 1 - \frac{nc_{vd}}{1 - c_{vd}} \right) \right] \quad (2-43)$$

The delivered concentration in the bend can be approximated using this formula, the wall shear stress is cancelled out of the equation. For vertical transport system this method will not be suitable since only a flow going up will be present. However, in the test setup VTS a similar section is present where 4 pressure measurements will be installed. The theory presented can be used to calculate the volumetric concentration in either the up-going or down-going section. When evaluating the pressure difference this will enable subtracting the static weight of the mixture, resulting in the pressure difference induced by wall shear stress.

## 2-7 Solids effect on Centrifugal Pumps

The drive behind the vertical transport is a set of booster stations, in these booster stations centrifugal pumps are installed of which the efficiency is affected by the slurry flow. The efficiency of a pump will decrease when a mixture containing settling solids is pumped. This effect is due to the slip velocity that exists between the solids and the fluid, thus decreasing the effect of the pump compared to the case where no solids are present. The efficiency of a centrifugal pump is expressed as:

$$\eta = \frac{Q_p \cdot p}{P} \quad (2-44)$$

Where  $Q[kg/m^3]$  is the volume flow,  $p_{man}[kpa]$  is the manometric pressure and  $P[W]$  is the power input. The efficiency decrease created by the settling solids can be expressed as a ratio between the efficiency when only fluid is pumped  $\eta_f$ , and the efficiency for mixture:

$$R_H = \frac{\eta_m}{\eta_f} \quad (2-45)$$

In 1965 a relation is defined that calculates this ratio using the volumetric concentration and the mass-median particle size ( $d_{50}$ ) by A.J. Stepanoff [20]:

$$R_h = 1 - c_v(0.8 + 0.6 \log(d_{50})) \quad (2-46)$$

This translates to the graph shown in figure 2-4, where the efficiency of the pump is shown with respect to the volumetric concentration and the mean diameter of the particles.

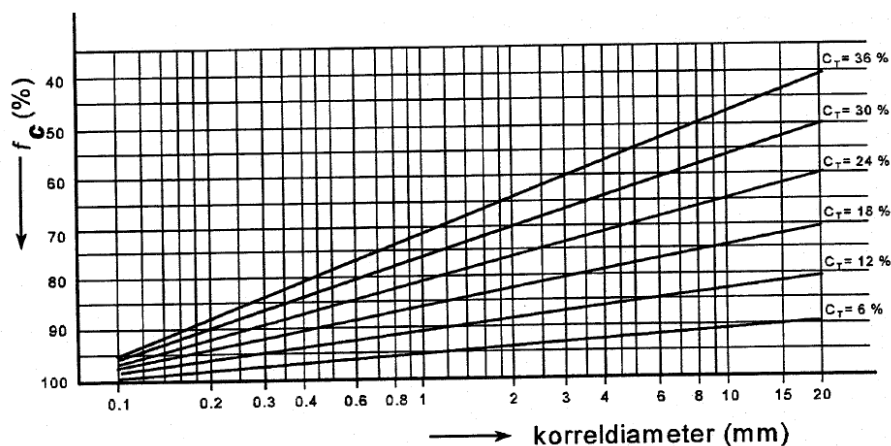


**Figure 2-4:** Pump efficiency with respect to the the volumetric concentration and the mean particle diameter, source: [21]

In figure 2-5 a different generalised solids-effect diagram for settling slurries is shown [22], this data was acquired empirically in the GIW Hydraulic Laboratory, and takes into account different impeller diameters and different grain sizes and a delivered concentration of 15%.

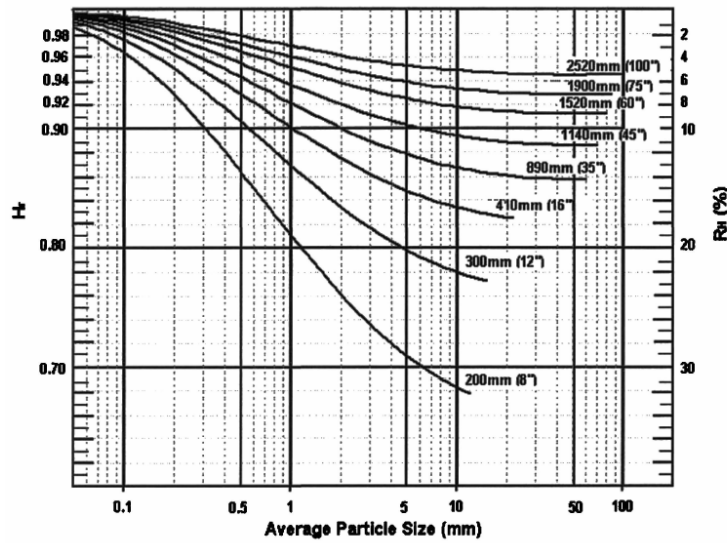


**Figure 2-5:** Pump efficiency with respect to the mean particle diameter and impeller diameter, source: [22]

The efficiency decrease scales linearly with the concentration for ( $c_v < 0.2$ ), using information and the presented data an equation has been created [23]:

$$R_H = 1 - \frac{c_v(0.466 + 0.4\log(d_{50}))}{D_{imp}} \quad (2-47)$$

Important to know for the observation of the concentration is the transformation of solid batches by pumps. It has been discovered that the influence of a pump performance on density waves transformation is negligible [21].

### 2-7-1 Discussion

Two formulas were presented relating the efficiency reduction of a centrifugal pump to the volumetric concentration and the median-mass particle diameter inside the pump. Both formulas are empirical relations and it is likely that the outcome will not be universal for all pumps. However, the formulas presented relate the particle diameter to the volumetric concentration which will be monitored, it will therefore be investigated whether the particle diameter can be determined by means of calculating the efficiency decrease of the pumps.

## 2-8 Nodule degradation

Currently under investigation at IHC is the degradation of nodules in the VTS. This includes degradation due to interparticle collision but also degradation due to interaction with the centrifugal pumps. It is investigated that the work of the pumps in the VTS have the largest impact on the particle size in the system [24]. Also it is concluded that smaller nodule particles are become less likely to break into smaller parts. IHC is still investigating the degradation

of nodule in order to predict a clear PSD transformation through the riser. The results of this investigation will be important for a monitoring system since the size of nodules affects the settling velocity of the nodules.

At the moment a method to estimate the settling velocity and particle diameter on-line is not yet developed and it is therefore recommended to investigate this first before taking into account any variation of settling velocity.

# Observer Algorithms

In this chapter observer algorithms are elaborated that are useful for the research problem. Furthermore a case is shown where an observer has been applied in the dredging industry before.

### 3-1 The filtering problem

Filtering is a challenge that is present in many processes, one wants to know all states defining a system while being able to measure only a part of them. The b1dVHT model will be used to observe solid concentrations in a riser, this means it is needed to look for a filter that can cope with high dimensions and non-linearity. For convenience the b1DVHT model is represented as follows:

$$\begin{aligned}\hat{x}_{k+1} &= f(\hat{x}_k, u_k) + w_k \\ y_k &= h(\hat{x}_k) + v_k\end{aligned}\tag{3-1}$$

The function  $f$  represents the non-linear function of the slurry model. The amount of states present in the system is defined as  $m$ , this number will be in the vicinity of 500. Process noise is defined as  $w_k$  and measurement noise as  $v_k$ , along with the following Gaussian distributions:

$$p(w) \sim N(0, Q)\tag{3-2}$$

$$p(v) \sim N(0, R)\tag{3-3}$$

In these distributions  $Q$  and  $R$  represent the model error covariance and the measurement error covariance respectively.

## 3-2 Kalman Filter

One of the most widely used state observe methods is the Kalman filter. The standard Kalman filter can only be applied to linear systems and will therefore not be suitable to the model presented. However, it forms the basis for a few types of observers that designed to work with non-linear systems. Therefore an explanation on the principles of the Kalman Filter will follow, an example linear system is defined as:

$$\begin{aligned}x_k &= Ax_{k-1} + Bu_k + w_k \\ y_k &= H_k x_k + v_k\end{aligned}\tag{3-4}$$

The Kalman filter steers the system in the right direction using feedback provided by the measurements. Two stages can be distinguished, the time update and the measurement update. In the time update the propagation of the state and model covariance is calculated, in the measurement update step the state is updated with the information from the measurement using the predicted covariance of the propagated state. The final step is updating the state covariance after the state has been updated with the measurement. The steps are shown below [25]:

Time update equations:

$$\bar{\hat{x}}_k = A\hat{x}_{k-1} + Bu_k\tag{3-5}$$

$$\bar{P}_k = AP_{k-1}A^T + Q\tag{3-6}$$

Measurement update equations:

$$K_k = \bar{P}_k H^T (H \bar{P}_k H^T + R)^{-1}\tag{3-7}$$

$$\hat{x}_k = \bar{\hat{x}}_k + K_k (y_k - H \bar{\hat{x}}_k)\tag{3-8}$$

$$P_k = (I - K_k H) \bar{P}_k\tag{3-9}$$

The Kalman filter has the potential to be the optimal filter for linear systems if the following conditions are satisfied:

- The model perfectly matches the real system
- The entering noise is white
- The covariances of the noise of the process and measurements are constant and known

In the real world very most systems do not satisfy to all these conditions. Extensions on the Kalman filter have been developed in order to make applications to non-linear systems possible, in the following sections these non-linear extensions are explained.

### 3-3 Extended Kalman Filter (EKF)

The Kalman filter presented is suitable for linear systems, however most systems are in fact non-linear. The Extended Kalman Filter incorporates non-linear behaviour by making a linearisation of the non-linear system, this results in a first order accurate filter. At the beginning of this chapter the form of our non-linear system is presented, the following Jacobians are defined based on that structure:

$$\begin{aligned} A &= \left. \frac{\partial f}{\partial x} \right|_{(\hat{x}_{k-1}, u_k, 0)} & W &= \left. \frac{\partial f}{\partial w} \right|_{(\hat{x}_{k-1}, u_k, 0)} \\ H &= \left. \frac{\partial h}{\partial x} \right|_{(\tilde{x}_k, 0)} & V &= \left. \frac{\partial h}{\partial v} \right|_{(\tilde{x}_k, 0)} \end{aligned} \quad (3-10)$$

These Jacobians are time-variant and are updated at every step. The matrices are used to incorporate the system's non-linear behaviour in the following state update approximations:

$$x_k \approx \tilde{x}_k + A(x_{k-1} - \hat{x}_{k-1}) + W w_{k-1} \quad (3-11)$$

$$y_k \approx \tilde{y}_k + H(x_k - \tilde{x}_k) + V v_k \quad (3-12)$$

In the same manner as is done with the standard Kalman filter, these equations lead to a time update and a measurement update:

Time update equations:

$$\bar{x}_k = f(\bar{x}_{k-1}, u_k, 0) \quad (3-13)$$

$$\bar{P}_k = A_k P_{k-1} A_k^T + W_k Q_{k-1} W_k^T \quad (3-14)$$

Measurement update equations:

$$K_k = \bar{P}_k H_k^T (H_k \bar{P}_k H_k^T + V_k R_k V_k^T)^{-1} \quad (3-15)$$

$$\hat{x}_k = \bar{x}_k + K_k (z_k - h(\bar{x}_k, 0)) \quad (3-16)$$

$$P_k = (I - K_k H_k) \bar{P}_k \quad (3-17)$$

When the gaussian probability distributions of the states are propagated through the non-linear functions the result is no longer gaussian distributed. This effect is not incorporated in the calculations of the EKF, which can lead to a poor representation of the non-linear function.

Another problem is the calculation of the Jacobians. The non-linear function of the 1DVHT transport model contains terms as the *modulus* and the *sign* of certain parameters. These terms cannot be incorporated in evaluating the Jacobian.

### 3-4 Particle filter

When the probability distribution through a non-linear function must be captured, a particle filter can be used. Particle filtering is a general Monte Carlo method for determining the propagation of states through a function. In different papers and works, different terms have been used to describe this filtering method. There are some minor differences in the different versions of the particle filter that are in use, but generally they are all based on the same principle: A set of point mass random samples with a probability density is used to generate the *a posteriori* density function [26].

As explained the non-linearity of the function causes the probability distribution of the states to be non-gaussian. It is thus required to construct the probability density function of the state using the collected output, this is expressed as  $p(x_k|y_{1:k})$ . Assuming  $p(x_0|y_0) = p(x_0)$  the prior probability can be obtained sequentially through prediction (Chapman-Kolmogorov Equation for the predictive distribution) [27]:

$$p(x_k|y_{1:k-1}) = \int p(x_k|x_{k-1})p(x_{k-1}|y_{1:k-1})dx_{k-1} \quad (3-18)$$

Using Baye's rule the measurement at time step  $k$  can be used to update the distribution:

$$p(x_k|y_{1:k}) = \frac{p(y_k|x_k)p(x_k|y_{1:k-1})}{p(y_k|y_{1:k-1})} \quad (3-19)$$

In order to retrieve the distribution the method of Sequential importance sampling (SIS) can be used. In this method the posterior distribution at time  $k-1$  is approximated using weighted samples of the states. These samples are called *particles* and are used to create the posterior distribution at time step  $k$ . The *a posteriori* distribution is approximated using importance sampling. The target distribution is generated by making use of a proposal distribution  $q(x)$ . If a function is created  $\pi(x)$  proportional to  $p(x)$ , sample weights can be made according to  $w_i \propto \pi(x^i)/q(x^i)$ . Then the *a posteriori* distribution is calculated as:

$$p(x_{0:k-1}|y_{1:k-1}) \approx \sum_{i=1}^N w_{k-1}^i \delta_{x_{0:k-1}^i} \quad (3-20)$$

The proposal distribution  $q(x)$  can be propagated through time to calculate it at every time step. It is assumed that  $q(x_k|x_{0:k-1}, y_{1:k}) = q(x_k|x_{k-1}, y_k)$ . This avoids the need of having to store all previous states. The following distribution and sample weights update can be derived:

$$\begin{aligned} x_k^i &\sim q(x_k|x_{k-1}^i, y_k) \\ w_k^i &\propto w_{k-1}^i \frac{p(y_k|x_k^i)p(x_k^i|x_{k-1}^i)}{q(x_k^i|x_{k-1}^i, y(k))} \end{aligned} \quad (3-21)$$

Described is a method to estimate the probability distributions of states, suitable for non-linear systems. However this method is very computational intensive which would be a problem for systems with a high dimension. Next filtering methods using the Monte Carlo method in a different way are described.

### 3-5 Unscented Kalman Filter (UKF)

Another method that incorporates the non-linear propagation of the states is the Unscented Kalman Filter. Using a minimal set of carefully chosen sample points (called sigma points) the true mean and covariance of the propagated state is determined.

The unscented Transformation is used to calculate the statistics of a random variable that undergoes a non-linear transformation. The following example demonstrates the propagation of a random variable  $x$  which has dimension  $m$  and covariance  $P_x$ . The mean of  $x$  is represented by  $\bar{x}$ . The non-linear function  $y = g(x)$  is evaluated. Based on  $\bar{x}$  the following *sigma vectors* are created which form the columns of matrix  $\chi$ .

$$\begin{aligned} X_0 &= \bar{x} \\ X_i &= \bar{x} + (\sqrt{(m + \lambda)P_x})_i, \quad i = 1, \dots, m \\ X_i &= \bar{x} - (\sqrt{(m + \lambda)P_x})_i, \quad i = m + 1, \dots, 2m \end{aligned} \quad (3-22)$$

All sigma vectors are then transformed through the non-linear equation:

$$Y_i = f(\chi_i) \quad (3-23)$$

For each sigma vector a weight is defined:

$$\begin{aligned} W_0^{(m)} &= \lambda / (m + \lambda) \\ W_0^{(c)} &= \lambda / (m + \lambda) + (1 - \alpha^2 + \beta) \\ W_i^{(m)} &= W_i^{(c)} = 1 / (2(L + \lambda)), \quad i = 1, \dots, 2m \end{aligned} \quad (3-24)$$

With  $\lambda$  defined as:

$$\lambda = \alpha^2(m + k) - m \quad (3-25)$$

The Unscented Transformation results in approximations that are accurate to the third order for Gaussian inputs for all nonlinearities. This unscented transformation can be used to create the so called *Unscented Kalman Filter*. For every time step the following set of equations are used to determine an estimate of the state:

$$X_{k-1}^a = [\hat{x}_{k-1}^a \quad \hat{x}_{k-1}^a \pm \sqrt{(L + \lambda)P_{k-1}^a}] \quad (3-26)$$

Time update equations:

$$X_k^x = f(X_{k-1}^x, X_{k-1}^w) \quad (3-27)$$

$$\hat{x}_k^- = \sum_{i=0}^{2L} W_i^{(m)} X_{i,k}^x \quad (3-28)$$

$$Y_k = H(X_k^x, X_{k-1}^v) \quad (3-29)$$

$$\tilde{y}_k^- = \sum_{i=0}^{2L} W_i^{(m)} Y_{i,k} \quad (3-30)$$

Measurement update equations:

$$P_{\tilde{y}_k \tilde{y}_k} = \sum_{i=0}^{2L} W_i^{(c)} (Y_{i,k} - \hat{y}_k^-)(Y_{i,k} - \hat{y}_k^-)^T \quad (3-31)$$

$$P_{x_k y_k} = \sum_{i=0}^{2L} W_i^{(c)} (X_{i,k} - \hat{x}_k^-)(Y_{i,k} - \hat{y}_k^-)^T \quad (3-32)$$

$$K = P_{x_k y_k} P_{\tilde{y}_k \tilde{y}_k}^{-1} \quad (3-33)$$

$$\hat{x}_k = \hat{x}_k^- + K(y_k - \hat{y}_k^-) \quad (3-34)$$

This method captures the non-linearity of the model without the need to evaluate a Jacobian or Hessian. It has been verified that the UKF consistently achieves a better level of accuracy than the EKF at a comparable level of complexity [28]. A problem of the UKF is the exponentially increasing number of calculations with respect to the number of states, this makes this method less suitable for high dimensional models.

### 3-6 Ensemble Kalman Filter (EnKF)

Another Kalman filter suitable for non-linear problems is the Ensemble Kalman Filter. This method is widely used for purposes regarding non-linear models of high order with uncertain initial states. An purpose where it is used very often is for example weather forecast simulations. Where at the UKF the sample points are chosen deterministically, the amount of samples (ensembles) for the EnKF is heuristic. This means that the distribution of the estimated state is not captured precisely, but often this method is precise enough. While one would expect that a large number of ensembles would be needed to obtain useful estimates, the literature on EnKF suggests that an ensemble of size 50 to 100 is often adequate for systems with thousands of states [29]. The computations for this method are described below.

For each timestep an ensemble of the forecasted state estimates is defined as matrix in  $\mathbb{R}^{n \times q}$ .

$$X_k^f = (x_k^{f1}, \dots, x_k^{fq}) \quad (3-35)$$

The number of the forecasted state estimates is represented by the superscript  $f_i$ . The ensemble mean is calculated as follows:

$$\bar{x}_k^f = \frac{1}{q} \sum_{i=1}^q x_k^{fi} \quad (3-36)$$

The mean of all ensemble members serves as the estimate of the new states. Since multiple ensembles are run at the same time the spread of the ensembles around the mean values of the ensemble is used to calculate the error covariance of the model. The error matrix around the ensemble means is defined:

$$E_k^f = [x_k^{f1} - \bar{x}_k^f, \dots, x_k^{fq} - \bar{x}_k^f] \quad (3-37)$$

$$E_{y_k}^f = [y_k^{f1} - \bar{y}_k^f, \dots, y_k^{fq} - \bar{y}_k^f] \quad (3-38)$$

The following approximations for the error covariance matrices are then calculated:

$$\hat{P}_{xy_k}^f = \frac{1}{q-1} E_k^f (E_{y_k}^f)^T \quad (3-39)$$

$$\hat{P}_{yy_k}^f = \frac{1}{q-1} E_{y_k}^f (E_{y_k}^f)^T \quad (3-40)$$

The Kalman gain for this filter can then be determined using the approximations for the error covariances. The estimated error covariance of the measurement is included as well.

$$\hat{K}_k = \hat{P}_{xy_k}^f (\hat{P}_{yy_k}^f + R)^{-1} \quad (3-41)$$

$$x_k^{a1} = x_k^{f1} + \hat{K}_k (y_k^i - h(x_k^{fi})) \quad (3-42)$$

These calculations can then be included in the following procedure:

Time update equations:

$$\hat{K}_k = \hat{P}_{xy_k}^f (\hat{P}_{yy_k}^f)^{-1} \quad (3-43)$$

$$x_k^{a_1} = x_k^{f_1} + \hat{K}_k (y_k^i - h(x_k^{f_i})) \quad (3-44)$$

$$\bar{x}_k^f = \frac{1}{q} \sum_{i=1}^N x_k^{f_i} \quad (3-45)$$

Measurement update equations:

$$x_{k+1}^{f_i} = f(x_k^{a_i}, u_k) + w_k^i \quad (3-46)$$

$$\bar{x}_k^f = \frac{1}{q} \sum_{i=1}^N x_k^{f_i} \quad (3-47)$$

$$E_k^f = [x_k^{f_1} - \bar{x}_k^f, \dots, x_k^{f_q} - \bar{x}_k^f] \quad (3-48)$$

$$E_{y_k}^f = [y_k^{f_1} - \bar{y}_k^f, \dots, y_k^{f_q} - \bar{y}_k^f] \quad (3-49)$$

$$\hat{P}_{xy_k}^f = \frac{1}{q-1} E_k^f (E_{y_k}^f)^T \quad (3-50)$$

$$\hat{P}_{yy_k}^f = \frac{1}{q-1} E_{y_k}^f (E_{y_k}^f)^T \quad (3-51)$$

The probability distribution of the estimated states is not captured deterministically, accuracy of the prediction is influenced by the chosen size of the ensemble. If a sufficiently large amount of ensembles is chosen the propagation of the states can be traced and a reduction of the computational power with respect to other particle filters can be achieved. In [29] it is concluded that the EnKF was used successfully for several non-linear applications once a suitable ensemble size was found.

The filter is a promising problem for the given purpose, however there are some aspects belonging to the EnKF to keep in mind when implementing this filter. They are elaborated in the following sections:

### 3-6-1 Undersampling

The amount of ensembles used is not determined and has to be chosen when designing the filter. The performance of the ensemble filter depends on the fact whether enough ensembles have been chosen. However a large ensemble size means a lot of computations which means the size cannot be chosen arbitrarily high. Undersampling is the case where too few ensembles have been chosen. Problems caused by this case are *inbreeding*, developing *long range spurious correlations* and *filter divergence* [30], which are explained in the following sections:

### 3-6-2 Inbreeding

Inbreeding is the situation where the analysis error covariances are systematically underestimated after each of the observation assimilations. This effect was first observed in [31]. The ensemble Kalman gain uses a ratio of the error covariance of the forecast background state and the error covariance of the observations to calculate to which extent the observation is trusted with respect to the forecast state. Using this gain the analysed state is determined.

If either the forecast error or observational error is incorrectly specified then the determination of the analysed state will be incorrect. The smaller the number of ensembles is, the greater the degree of undersampling is present and the greater the chance is of underestimated forecast error covariances, or inbreeding. Inbreeding is a potential source of *filter divergence* and the development of *long range spurious correlations* [30].

### 3-6-3 Spurious Correlations

Spurious correlations occur when the state variables are updated by measurements that are made at another state. If the number of ensembles is low, the model error covariance is overestimated. This effect is stronger for measurements that are far away from the measurements. These far away states will have a larger spread and thus a larger estimated error covariance. This aspect causes that they are affected by the measurements more, even if the measurement is at a far away location.

A technique to avoid the spurious correlations is called *localisation*. A field ( $\rho \mathbb{R}^{m \times m}$ ) is created indicating which states can be affected by other states, in the case of the VTS these are the neighbouring states defined by a cutoff length  $c$ . The localisation field is multiplied with the covariance matrix using the Hadamard product and the kalman gain then becomes:

$$\hat{K}_k = \rho \circ \hat{P}_{xy_k}^f (\hat{P}_{yy_k}^f)^{-1} \quad (3-52)$$

Gaspari-Cohn's fifth-order polynomial function [32] can be used to create the localisation field  $\rho$ , this field is constructed as:

$$\rho(c) = \begin{cases} -\frac{1}{4}c^5 + \frac{1}{2}c^4 + \frac{5}{8}c^3 - \frac{5}{3}c^2 + 1, & \text{if } 0 \leq c \leq 1 \\ \frac{1}{12}c^5 - \frac{1}{2}c^4 + \frac{5}{8}c^3 + \frac{5}{3}c^2 - 5c + 4 - \frac{21}{3c}, & \text{if } 1 < c \leq 2 \\ 0, & \text{if } c > 2 \end{cases} \quad (3-53)$$

In this equation  $c = \frac{\Delta L}{c_l}$ ,  $c_l$  is the cut-off length and  $\Delta L$  is the distance between two states.

### 3-6-4 Filter divergence

Filter divergence occurs when the analysed state moves away from the true state and can no longer be corrected by the observations [30]. If during observations the covariance of the forecast estimate is small a high weight is placed on the forecast estimate and low weight is placed on the observations. As the size of the analysis covariances decreases this effect

will continue diminishing the influence of the measurements. The standard deviation of the analysis state ensemble is smaller than that of the forecast state ensemble and the the ensemble members will converge.

At the end due to the very low estimated covariance the measurements have no longer effect on the states of the system. The filter can no longer steer the incorrect estimates of the states in the direction of the real state. When this has happened divergence has occurred. A mitigation for this problem is found. It is called *inflation*. At each time step the error covariance matrix of the states is multiplied by a constant factor  $r$ . This factor usually is between 1.01 and 1.20. In this way, in this way the estimated error covariance is increased to counteract the underestimated covariance.

### 3-7 Unknown Input Observer

Since the particle diameter is identified as an unknown input of the system, literature is elaborated which can be relevant for estimating this particle.

An observer type designed for systems with an unknown input is the Unknown Input Observer, a definition of an unknown input observer is that the state estimate converges to the real state when the input is not known. This does not necessarily mean that the input is observed as well. An input observer structure for linear systems is elaborated in [33], where the following model structure was used for the linear system:

$$\begin{aligned}x[k + 1] &= Ax[k] + Bu[k] \\y[k] &= Cx[k] + Du[k]\end{aligned}\tag{3-54}$$

In this model the state vector is  $x \in \mathbb{R}^m$  and the input  $u \in \mathbb{R}^n$ . The output can be defined as:

$$y[k : k + L] = O_L x[k] + J_L u[k : k + L]\tag{3-55}$$

An observer is then created in the form:

$$\hat{x}[k + 1] = E\hat{x}[k] + Fy[k : k + L]\tag{3-56}$$

Where  $L$  is the delay of the observer caused by the fact that the input is unknown. A design procedure is elaborated based on the assumption that  $\begin{bmatrix} B \\ D \end{bmatrix}$  is full rank, started is with solving:

$$N \begin{bmatrix} D & 0 \\ O_{L-1}A & J_{L-1} \end{bmatrix} = \begin{bmatrix} 0 & 0 \\ I & 0 \end{bmatrix}\tag{3-57}$$

Then choose the matrix  $\hat{F}_1$  in a way that the eigenvalues of  $E = (A - BS_2) - \hat{F}_1 S_1$  are stable and satisfy:  $F = [\hat{F}_1 B]N$ . The observer is then designed, if the following is solved:

$$G \begin{bmatrix} B \\ D \end{bmatrix} = I \quad (3-58)$$

An estimation of the inputs can be retrieved:

$$\hat{u}(k) = G \begin{bmatrix} \hat{x}(k+1) - A\hat{x}[k] \\ y[k] - C\hat{x}[k] \end{bmatrix} \quad (3-59)$$

Two conditions need to be evaluated in order to know if this observer can be made:

$$\text{rank}(J_L) - \text{rank}(J_{L-1}) = n \quad (3-60)$$

and:

$$\text{rank} \begin{bmatrix} A - zI & B \\ C & D \end{bmatrix} = n + m, \quad \forall z \in C, |z| \leq 1, \quad (3-61)$$

### 3-8 Simultaneous Input and State Filtering (SISF)

A different method has been described which enables simultaneous input and state filtering based on the Ensemble Kalman filter [34]. Based on the observed output the model and output are corrected using a Bayesian statistical framework, this algorithm does not need a model for the input.

For this algorithm the unknown input is added to the state vector  $x$ , for systems without feedthrough of the input to the output the following algorithm is presented (EnSISF-w/oDF) as pseudo-code:

1. for  $k = 1 : k_{end}$
2.     Generate  $\hat{u}^l(k-1)$
3.     for  $l = 1 : l_{max}$
4.         Repeat equations 3-52 - 3-51 of the Ensemble Kalman filter
5.         export  $\hat{u}^l(k)$
6.     end
7.     export  $\hat{u}^{l_{max}}(k)$  and  $\hat{x}(k)$
8. end

At every time step the Enkf algorithm is iterated  $l$  times and after every iteration only the input state  $u$  is stored and reused for the next iteration. In this way the the input is iterated, and the state update is repeated using the updated input. At the last iteration both state and input estimation are used and stored.

The augmented EnKF has been applied to the simulation of the Lorenz'96 model and on wildfire simulation based on a real wildfire data. For these situations both states and input were estimated simultaneously. A remark however is that the input needs to be observable from the output in order to use this algorithm.

### 3-9 Observers in Slurry Transport

An observer applied on slurry transport is elaborated in this section. It has been found before that when observing a slurry flow, the partice diameter is important. Usually this input depends on the local conditions of the soil that is collected which means it is not at all times known. This information may be unknown, however based on measurements in the slurry flow this parameter might be possible to be measured. It is described in [35] that for observing, an uncertain parameter without a model can be described as a random walk model. For the case of the  $d_m$  this would yield:

$$dd_m(t) = 0dt + de(t) \quad (3-62)$$

In this formula  $e$  is a Wiener process with a standard deviation  $\sigma$ . This example has been found in [36], in that thesis the mean particle diameter was estimated using this method. The method was applied to a dredging hopper, using simulations.

In [37] four observation problems regarding dredging have been described: estimating the mean particle size of the dredged soil, estimating the overflow losses of a hopper, estimating the dredging forces and estimating the anchor positions of a vessel. The goal of the research has been to optimize the dredging process, interesting for this survey is the estimation of the mean grain size of the dredged material.

In the research the mean particle diameter has been determined using the mixture flow, mixture density and the discharge pressure in a pipeline. The conditions needed is that the pipe length and geometrics are well known. The used model is usable to estimate solids with a grain size ranging up to 3mm. The model for the calculation of the flow in the discharge-pipeline can be described by the second-law of dynamics:

$$\dot{Q}_p = \frac{S}{\rho \cdot L} (H_{disc} - \Delta H_m - \rho_m) \quad (3-63)$$

In this equation  $\rho_m$  is the density of the outgoing mixture,  $S$  is the discharge-pipeline section,  $H_f$  is the pressure loss in the pipeline. Where the head loss is described as:

$$\Delta H_m = \alpha \frac{\rho_m}{\rho_f} \Delta H_f + (1 - \alpha) \left( 1 + 2 \left( \frac{v_{crit}}{v} \right)^3 \right) \Delta H_f \quad (3-64)$$

Where  $\alpha$  is a weighing factor between 0 and 1. The critical speed is defined according to the formula of Jufin-Lopatin [38]:

$$v_{crit} = \sqrt[3]{\frac{1}{2} \cdot c_v \cdot 33000 \cdot (g \cdot d)^{\frac{3}{2}} \frac{d_m}{d}} \quad (3-65)$$

A system is defined as:

$$x = \begin{bmatrix} Q \\ d_m \\ \alpha \end{bmatrix}, y = [Q] \quad (3-66)$$

An Extended Kalman Filter has been used to observe the particle diameter, experimental data of a Cutting Suction Dredger has been used to verify the results and the results were successful. The grain diameter has been measured within a relative error of  $\approx 10\%$ .

In [36] the estimation of the particle diameter in a trailing suction dredger hopper is described as well, in this research a more complicated method has been used which is applied to a hopper vessel. In the model it is assumed that the height of the sand bed, the total height of the mixture, the total mass of the mixture, the incoming flow rate and the incoming flow density can be measured. Bed and mixture height and mass are states of the system. The average particle diameter is modelled as a state without a model with added noise. The mass of the solids and the height of the solid bed are related tot the mean grain diameter through a non-linear function. Multiple observer types have been compared. It has been concluded that for different phases of the hopper filling process different observers are optimal.

Both situations are different than the situation of the VTS, the effect of the solid size is harder to measure on the pressure drop in a vertical section and furthermore the literature evaluated only covers estimation of grain sizes with small diameters. However, the approaches have in common that that the particle diameter is described as a modelless parameter, and is observed using non-linear relations to the measurable parameters.

### 3-10 Cascade observers

Observers can be decoupled into multiple observers of which the output connects to the next observer. The performance of these so called *cascade observers* is investigated [39]. Decoupling an observer into different types of observers has the advantage of using the strength of different observer types. It was shown that the distributed Kalman filters can be jointly optimal, if and only if the subsystems are independent.

Different cascade Kalman filters were tested, it was conluded that the performance of this setup is comparable to a centralized Kalman filter. Two applications were tested of which one is the hopper model from the previous section. The performance of the cascade observers is concluded to be comparable to that of the centralized observer. Furthermore the configuration enables that the observers can be tuned more easily.



---

# Chapter 4

---

## Conclusion

Relevant literature has been analysed about vertical hydraulic transport and observer algorithms, in this sections conclusions for the research are elaborated.

### 4-1 Vertical Hydraulic Transport

A model suitable for simulating vertical Hydraulic transport of solids in a riser is the 1DVHT model, this model has been validated using an experiment but is too computationally intensive to run real-time. A basic version was created (b1DVHT model) which is suitable for use in an online observer, it has been proven that the model yields similar results.

An important parameter of the slurry is the particle diameter, this parameter determines the settling velocity and is therefore important for determining the velocity of solids propagating through the riser. The model of Ferguson and Church is valid under the conditions of the test setup and is therefore still valid to be used in the b1DVHT model, however since the hindered settling velocity is a combination of multiple researches it is expected that the literature may deviate from experiments in reality.

Literature about the hydraulic gradient of mixtures was evaluated since the pressure drop will be used to determine the volumetric concentration inside the riser. In literature the hydraulic gradient is subdivided into a term for potential energy, a term for the friction induced by the fluids and a term that represents the presence of solids. For the contribution of solids multiple theories were evaluated. No model was found covering the whole range of solids that will be tested, which is why multiple theories need to be evaluated in order to find the best match with the performed measurements.

Literature was found about the efficiency decrease of centrifugal pumps, related to the particle diameter. This gives an option to determine the particle diameter: Using the test setup it can be investigated whether the particle diameter can be determined by measuring the efficiency decrease of the pump.

## 4-2 Observer Algorithms

Different observing techniques have been investigated. The most common observer is known to be the Kalman filter, this filter itself is not applicable for the requested properties, however many extensions have been created. Monte Carlo based methods provide solutions that do no longer require the calculation of a Jacobian, probability distributions representing the error covariance of the model can be estimated using selected random samples. This is convenient for the 1DVHT model of which the Jacobian cannot be evaluated. If the model error covariance does not need to be determined deterministic the EnKF appears to be a suitable observation method. The computational power requested is low compared to filters as the UKF and the Enkf has proven itself in multiple high dimensional applications. Problems described in literature are related to stability, it is concluded that it is very important that a right ensemble size needs to be selected. Furthermore a method to avoid spurious correlations between states is found.

For vertical transport no method was found in literature suitable for determining the particle diameter which is the unknown input of the system considered. As is elaborated the particle diameter can be identified using the pressure drop in a vertical pipe section, with this it was shown how an unknown input can be observed using physical relations, however this method is not suitable for vertical pipe sections. A possible method to observe the particle diameter is thus to design a model from which the particle diameter can be observed in VTS. A different method to observe the particle diameter is by means of Sequential Input and Output Filtering, using this method the algorithm of the Enkf is used in order to observe the input by performing iterations. This method may be promising if the particle diameter can be observed from a defined output, an observability analysis therefore needs to be performed.

Cascade filters can be used to combine the strength of different observers. For the observation of the concentration the Ensemble Kalman filter is selected, however for different parameters as the particle diameter other observer structures can be used.

---

# Bibliography

- [1] “Polymetallic Nodules,” *International seabed authority*, pp. 1–8, 2006.
- [2] M. van Dort, *Monitoring of the slurry density along the length of the VTS*. MSc Thesis, Tu Delft.
- [3] J. van Wijk, *Vertical Hydraulic Transport for deep sea mining*. PhD thesis, Tu Delft.
- [4] U. Zanke, “Berechnung der Sinkgeschwindigkeiten von Sedimenten,” *Mitteilungen des Franzius-Institutes*, 1977.
- [5] R. I. Ferguson and M. Church, “A simple universal equation for grain settling velocity,” *Journal of Sedimentary Research*, vol. 74, no. 6, pp. 933–937, 2000.
- [6] P. N. Rowe, “A convenient empirical equation for estimation of the Richardson-Zaki exponent,” *Chemical Engineering Science*, 1987.
- [7] J. Richardson and W. Zaki, “Sedimentation and fluidisation: Part I,” *Chemical Engineering Research and Design*, vol. 75, no. 3, pp. S82–S100, 1997.
- [8] P. H. Borchert, “The Influence of Metal Content on the Physical and Mineralogical Properties of Pelagic Manganese Nodules,” vol. 1, 1975.
- [9] W. Boomsma, N. Ostergaard, P. Verduyn, A. Mitzlaff, L. Rattmann, G. Nicholson, K. Green, and J. Warnaars, “Terms of Reference for VTS design Confidential,” tech. rep., European Commission Seventh Framework Programme NMP-2013.4.1-2 GA, 2014.
- [10] P. K. Swamee and A. K. Jain, “Explicit equations for pipe-flow problems,” *Journal of Hydraulic Division, ASCE*, vol. 102, no. 5, pp. 657–664, 1976.
- [11] S. A. Miedema, *Slurry Transport: Fundamentals, a Historical Overview and The Delft Head Loss & Limit Deposit Velocity Framework*. 2016.
- [12] C. A. Shook and A. S. Bartosik, “Particle-wall stresses in vertical slurry flows,” vol. 81, pp. 117–124, 1994.

- [13] V. Matoušek, "Pipe-wall friction in vertical sand-slurry flows," *Particulate Science and Technology*, vol. 27, no. 5, pp. 456–468, 2009.
- [14] A. Bartosik, "Influence of Coarse-Dispersive Solid Phase on the "Particles-Wall" Shear Stress in Turbulent Slurry Flow with High Solid Concentration," *The Archive of Mechanical Engineering*, vol. LVII, no. 1, 2010.
- [15] J. R. Ni, "Hydraulic Lifting of Manganese Nodules Through a Riser," vol. 126, no. February 2004, pp. 72–77, 2017.
- [16] Wang G. Q. and Fei X. J., "No Title," *Proc. of Fourth International Symposium on River Sedimentation*, pp. 1459–1466, 1989.
- [17] J. X. Xia, J. R. Ni, and C. Mendoza, "Upward Flow of Large Size Particles in Water Mixtures through Swaying Pipes," no. August, pp. 535–544, 2004.
- [18] "Blue Mining Task 4.5.2 Validation Of Codes For Dynamic Analysis Of The Deep Sea Mining System," tech. rep., European Commission Seventh Framework Programme NMP-2013.4.1-2 GA, 2016.
- [19] R. Clift and D. H. Manning Clift, "Continuous measurement of the density of flowing slurries," *International Journal of Multiphase Flow*, vol. 7, no. 5, pp. 555–561, 1981.
- [20] A. Stepanoff, *Pumps and Blowers, Two-Phase Flow: Selected Advanced Topics*. J. Wiley, 1965.
- [21] V. Matoušek, *Dredge Pumps and Slurry Transport*. 2004.
- [22] K. C. Wilson, G. R. Addie, A. Sellgren, and R. Clift, *Slurry Transport Using Centrifugal Pumps*. 2006.
- [23] S. A. Miedema, "Considerations on limits of dredging processes," 1994.
- [24] J. Zenhorst, "Degradation of poly-metallic nodules in a dredge pump Delft University of Technology Degradation of poly-metallic nodules in a dredge pump," 2016.
- [25] G. Welch and G. Bishop, "An Introduction to the Kalman Filter," *In Practice*, vol. 7, no. 1, pp. 1–16, 2006.
- [26] E. Orhan, "Particle filtering," no. 1, pp. 1–6, 2012.
- [27] M. S. Arulampalam, S. Maskell, N. Gordon, and T. Clapp, "A Tutorial on Particle Filters for Online Nonlinear / Non-Gaussian Bayesian Tracking," vol. 50, no. 2, pp. 174–188, 2002.
- [28] E. Wan and R. Van Der Merwe, "The unscented Kalman filter for nonlinear estimation," *Proceedings of the IEEE 2000 Adaptive Systems for Signal Processing, Communications, and Control Symposium (Cat. No.00EX373)*, pp. 153–158, 2002.
- [29] S. Gillijns, O. Mendoza, J. Chandrasekar, B. De Moor, D. Bernstein, and A. Ridley, "What is the ensemble Kalman filter and how well does it work?," *2006 American Control Conference*, p. 6 pp., 2006.

- 
- [30] R. E. Petrie, *Localization in the ensemble Kalman Filter*. No. August, MSc Thesis, University of Reading, 2008.
- [31] P. L. Houtekamer and H. L. Mitchell, “Data assimilation using an ensemble Kalman filter technique,” *Monthly Weather Review*, vol. 126, no. 3, pp. 796–811, 1998.
- [32] G. Gaspari and S. E. Cohn, “Construction of Correlation Functions in Two and Three Dimensions,” *Quarterly Journal of the Royal Meteorological Society*, vol. 125, no. 554, pp. 723–757, 1999.
- [33] S. Sundara, *Observers for Linear Systems with Unknown Inputs*. MSc Thesis, University of Waterloo, 2003.
- [34] H. Fang, T. Srivas, R. A. de Callafon, and M. A. Haile, “Ensemble-based simultaneous input and state estimation for nonlinear dynamic systems with application to wildfire data assimilation,” *Control Engineering Practice*, vol. 63, no. April, pp. 104–115, 2017.
- [35] G. Kitagawa, “A Self-Organizing State-Space Model,” *Taylor & Francis*, vol. 93, no. 443, pp. 1203–1215, 2017.
- [36] P. M. Stano, *Nonlinear State and Parameter Estimation for Hopper Dredgers*. PhD thesis, Tu Delft.
- [37] J. Braaksma, J. Osnabrugge, and C. De Keizer, “Estimating the Immeasurable: Soil Properties,”
- [38] A. P. Jufin and N. A. Lopatin, “O projekte TUiN na gidrotransport zernistych materialov po stalnym truboprovodam,” *Gidrotechniceskoe Strojitelstvo*, pp. 49–52, 1966.
- [39] Z. Lendek, R. Babuška, and B. de Schutter, “Distributed Kalman filtering for cascaded systems,” *Engineering Applications of Artificial Intelligence*, vol. 21, no. 3, pp. 457–469, 2008.



---

# Glossary

## List of Symbols

### Abbreviations

1DVHT	1-Dimensional Vertical Hydraulic Transport
b1DVHT	Basic 1-Dimensional Vertical Hydraulic Transport
EKF	Extended Kalman Filter
EnKF	Ensemble Kalman Filter
VTs	Vertical Transport System

### Greek Symbol

$\epsilon$	Pipe-wall roughness	[–]
$\eta$	Pump efficiency	[–]
$\lambda$	Linear concentration	[–]
$\nu_f$	Kinematic viscosity	[ $m^2/s$ ]
$\rho$	Localisation field	[ $kg/m^3$ ]
$\rho$	Localization field	[–]
$\rho_f$	Fluid density	[ $kg/m^3$ ]
$\rho_m$	Mixture density	[ $kg/m^3$ ]
$\rho_s$	Solid density	[ $kg/m^3$ ]
$\tau_f$	Fluid wall shear stress	[ $Pa$ ]
$\tau_m$	Mixture wall shear stress	[ $Pa$ ]
$\tau_s$	Solid wall shear stress	[ $Pa$ ]
$c_{vmax}$	Maximum concentration	[–]
$d$	Particle diameter	[ $m$ ]
$v_{crit}$	Critical velocity	[ $m/s$ ]
$X$	Sigma matrix	[–]

**Roman symbol**

$\bar{v}_m$	Mixture bulk velocity	[ <i>m/s</i> ]
$A_p$	Cross section of pipe	[–]
$Ba$	Bagnold's number	[–]
$c$	cut-off length	[–]
$c_l$	Cut-off length	[–]
$c_v$	Volumetric concentration	[–]
$D$	Pipe diameter	[ <i>m</i> ]
$d_r$	Representative diameter	[ <i>m</i> ]
$d_{50}$	Mass-mean particle size	[ <i>m</i> ]
$d_m$	Mean Particle Diameter	[ <i>m</i> ]
$f_D$	Darcy-Weisbach friction factor	[ <i>Pa</i> ]
$g$	Gravitational Constant	[ <i>m/s</i> <sup>2</sup> ]
$h$	Output function	[–]
$i_f$	Hydraulic gradient due to fluid wall shear stress	[–]
$i_p$	Hydraulic gradient due to potential energy	[–]
$i_s$	Hydraulic gradient due to solid wall shear stress	[–]
$i_t$	Total hydraulic gradient	[–]
$k$	Time step	[–]
$m_i$	Mass of particle	[ <i>kg</i> ]
$n_{rz}$	Richardson and Zaki exponent	[–]
$P$	Power supply	[ <i>W</i> ]
$p$	Probability distribution	[ <i>m/s</i> ]
$p_{man}$	Manometric pressure	[ <i>pa</i> ]
$Q$	Model error covariance matrix	[–]
$q$	Proposal distribution	[ <i>m/s</i> ]
$Q_p$	Volume flow	[ <i>m</i> <sup>3</sup> / <i>s</i> ]
$R$	Measurement covariance matrix	[–]
$R_H$	Efficiency decrease of pump	[–]
$Re$	Reynolds number	[–]
$Re_p$	Particle Reynolds number	[ <i>m</i> ]
$Stk$	Stokes number	[–]
$u_*$	Shear velocity	[ <i>m/s</i> ]
$v$	Measurement noise	[–]
$v_f$	Fluid velocity	[ <i>m/s</i> ]
$v_s$	Solid velocity	[ <i>m/s</i> ]
$w$	Model noise	[–]
$w_h$	Hindered settling velocity	[ <i>m/s</i> ]
$w_t$	Terminal settling velocity	[ <i>m/s</i> ]
$x$	State vector	[–]
$y$	Output vector	[–]
$z$	Height	[ <i>m</i> ]